ChemComm

FEATURE ARTICLE

View Article Online
View Journal | View Issue

Open Access Article. Published on 02 2025. Downloaded on 06.02.2026 19:38:33.
This article is licensed under a Creative Commons Attribution 3.0 Unported Licence.

Check for updates

Cite this: *Chem. Commun.*, 2025, **61**, 11118

Raman optical activity of amyloid fibrils: a distinctive chiroptical phenomenon beyond resonance

Aleksandra Kołodziejczyk,[ab] Aleksandra Wajda*[a] and Agnieszka Kaczor*[a]

Received 30th April 2025,
Accepted 9th June 2025

DOI: 10.1039/d5cc02442k

rsc.li/chemcomm

Raman optical activity (ROA) exhibits dual characteristics for analysis of biological systems. Despite its excellent stereosensitivity and ability to study samples in aqueous solutions, the weak ROA signals limit its applicability in the case of biological samples, for which analyte concentrations are typically low. Therefore, there is considerable interest in developing techniques to enhance ROA signals. Most of the proposed approaches, which we review here, exploit a certain form of resonance. Against this background, we discuss a newly observed phenomenon, namely, the exceptionally intense ROA signals of amyloid fibrils, focusing on the nature of this effect, future works necessary to confirm its origin and its potential utility in the analysis of amyloid fibrils.

1. Introduction

The phenomenon of chirality has fascinated and puzzled scientists since its first observation. This has led to a search for efficient tools that allow one to explore the chiral world. However, it has not been the simplest task, as many 'classic' techniques are 'blind' in terms of chirality or have limitations, such as the requirement of crystallization in the case of X-ray crystallography. An important step in the advancement of studying chiral systems was the development of chiroptical techniques, which are, in principle, based on the different interactions of optically active molecules with left- and right-circularly polarized light. Based on the type of energy transition

[a] *Faculty of Chemistry, Jagiellonian University, 2 Gronostajowa Str., 30-387 Krakow, Poland. E-mail: aleksandra.wajda@uj.edu.pl, agnieszka.kaczor@uj.edu.pl*
[b] *Doctoral School of Exact and Natural Sciences, Jagiellonian University, 11 Lojasiewicza Str., 30-348 Krakow, Poland*

Aleksandra Kołodziejczyk

Aleksandra Kolodziejczyk is a doctoral student at the Faculty of Chemistry, Jagiellonian University in Krakow (JU), Poland. In 2022 she obtained an MSc degree in medicinal chemistry at the same university. Since her undergraduate studies, she has been involved with the Chiroptical Spectroscopy Group at JU, where she now conducts her doctoral research. Her interests center on chiral supramolecular systems and enhancement of chiral signals. She is currently engaging in research related to amyloid fibrils, focusing on their chiral properties and application of chiroptical spectroscopies (particularly vibrational optical activity) to investigate these fascinating proteinaceous systems.

Aleksandra Wajda

Aleksandra Wajda is a post-doctoral researcher at the Faculty of Chemistry, Jagiellonian University, specializing in chiroptical spectroscopy of supramolecular systems, particularly amyloid fibrils. She earned her PhD in materials engineering in 2018 from AGH University of Science and Technology. Her research focuses on vibrational optical activity methods such as Raman optical activity and vibrational circular dichroism to study chirality and polymorphism in biomolecular assemblies. She also develops spectroscopic tools for clinical diagnostics, including Raman- and FTIR-based evaluation of red blood cell concentrates. Her interdisciplinary work integrates spectroscopy, materials science, and cell biology to support advanced biomedical applications.

 This journal is © The Royal Society of Chemistry 2025

Open Access Article. Published on 02 2025. Downloaded on 06.02.2026 19:38:33.
This article is licensed under a Creative Commons Attribution 3.0 Unported Licence.

two main types of chiroptical spectroscopy can be distinguished—vibrational (VOA) and electronic optical activity (EOA), with the main techniques being vibrational circular dichroism (VCD) and Raman optical activity (ROA) for VOA, and electronic circular dichroism (ECD), optical rotatory dispersion (ORD), and circularly polarized luminescence (CPL) for EOA.[1,2]

Chiroptical spectroscopies have been used to address problems such as the determination of absolute configuration and enantiomeric excess[3–5] and have also become essential tools for studying biomolecules.[6] Despite the advancements made in the field in the last few decades and increasing availability of commercial instruments having contributed to the growing interest in chiroptical methods, their potential is still not fully explored.

Among the techniques with great potential that are yet to reach their prime is ROA. ROA is based on the detection of the small difference in the intensity of Raman scattering of left and right components of circularly polarized light.[1,2] It was first theoretically described in 1969 by Atkins and Barron[7] and was further developed two years later by Barron and Buckingham, who introduced a dimensionless circular intensity difference (CID), defined as the ratio of ROA-to-Raman intensity.[8] Among other chiroptical techniques, ROA is a particularly promising candidate for studying chiral and biologically relevant samples in solution. The main advantage of ROA is that it enables measurements in aqueous environments, due to the relatively weak Raman signal of water in the 0–3000 cm^{-1} region, which does not interfere with the sample spectra, unlike VCD. Moreover, ROA spectra are richer in bands and are better resolved compared to ECD. Since the first experimental confirmation by Barron *et al.* in 1973[9] and introduction of a commercially available spectrometer (2003, BioTools),[10] ROA has been used to study a vast range of molecules, including saccharides,[11,12] nucleic acids, proteins, and even viruses[13–15] as well as inorganic compounds, including metal complexes.[16,17] A constant effort is also being made to advance the ROA instrumentation, aiming to broaden the implementation of the technique.

Agnieszka Kaczor

Agnieszka Kaczor is a professor at the Faculty of Chemistry, Jagiellonian University (JU), Poland. From there, she received her PhD in 2003 and then did two years postdoctoral research at the University of Coimbra, Portugal. Since returning to Poland, she has been associated with the Faculty of Chemistry, JU where, from 2020, she has been leading the Chiroptical Spectroscopy Group. Her current research focuses on chiral supramolecular systems, particularly biogenic, self-assembling structures, amplification and induction of chirality, enantiorecognition as well as mechanisms of signal enhancement in vibrational optical activity.

Despite that, the use of ROA remains limited, with one of the main drawbacks being the weak signal. Compared to Raman, the intensity of ROA bands is typically three or four orders of magnitude smaller, thus resulting in the requirement of large concentrations, high laser power (up to few hundred mW) and long acquisition times (up to days). This limitation is a fundamental reason why scientists are on the lookout for various strategies aimed at amplifying the ROA signal. At the same time, systems that could provide intense ROA are also of high interest. Among the most intriguing findings is the exceptionally strong ROA signal from amyloid fibrils recently reported by our group.[18] This phenomenon raises fundamental questions about the structural and morphological features responsible for ROA enhancement and opens new possibilities for applying ROA in biomedical research.

The purpose of this feature article is to discuss the ROA of amyloid fibrils and its future perspectives in the broader context of ROA enhancement. First, we look at the most common method of ROA enhancement through resonance, while discussing possible problems with such measurements. We provide examples of systems exhibiting resonance ROA (RROA), with focus on retinoids and carotenoid aggregates. Next, we briefly introduce novel, state-of-the-art methods such as surface-enhanced (SERROA) and coherent (CARS-ROA) ROA.

The final section is devoted to the topic of amyloid fibrils, their structure, ROA spectra, and complementarity of different chiroptical methods in the study of amyloids. Ultimately, we discuss various aspects and concerns regarding exceptionally intense ROA of amyloid fibrils and perspectives in using ROA to study proteinaceous aggregates in the future.

2. Methods of signal enhancement involving resonance

To date, most systems that generate unusually intense ROA take advantage of a certain form of resonance. These approaches are discussed here beginning with simpler ones and progressing toward more specialized and state-of-the-art methods (Fig. 1).

2.1. Resonance Raman optical activity

One of the simplest methods for increasing the intensity of ROA is to couple the excitation energy with the electronic transition energy of the analyte. This method, considered the chiral equivalent of resonance Raman spectroscopy, is known as RROA. The theory of RROA, developed by Laurence Nafie, initially accounting for the contribution of a single excited electronic state (SES-RROA[19]), was later extended to consider two electronic states.[2] Resonance through a single electronic state results in a very unique form of RROA, that is monosignated (of either negative or positive sign) and mirrors the relative intensities of the parent Raman spectrum.[19]

Additionally, it is interrelated with ECD that for scattered circular polarization (SCP) mode in backscattering is described

Open Access Article. Published on 02 2025. Downloaded on 06.02.2026 19:38:33.
This article is licensed under a Creative Commons Attribution 3.0 Unported Licence.

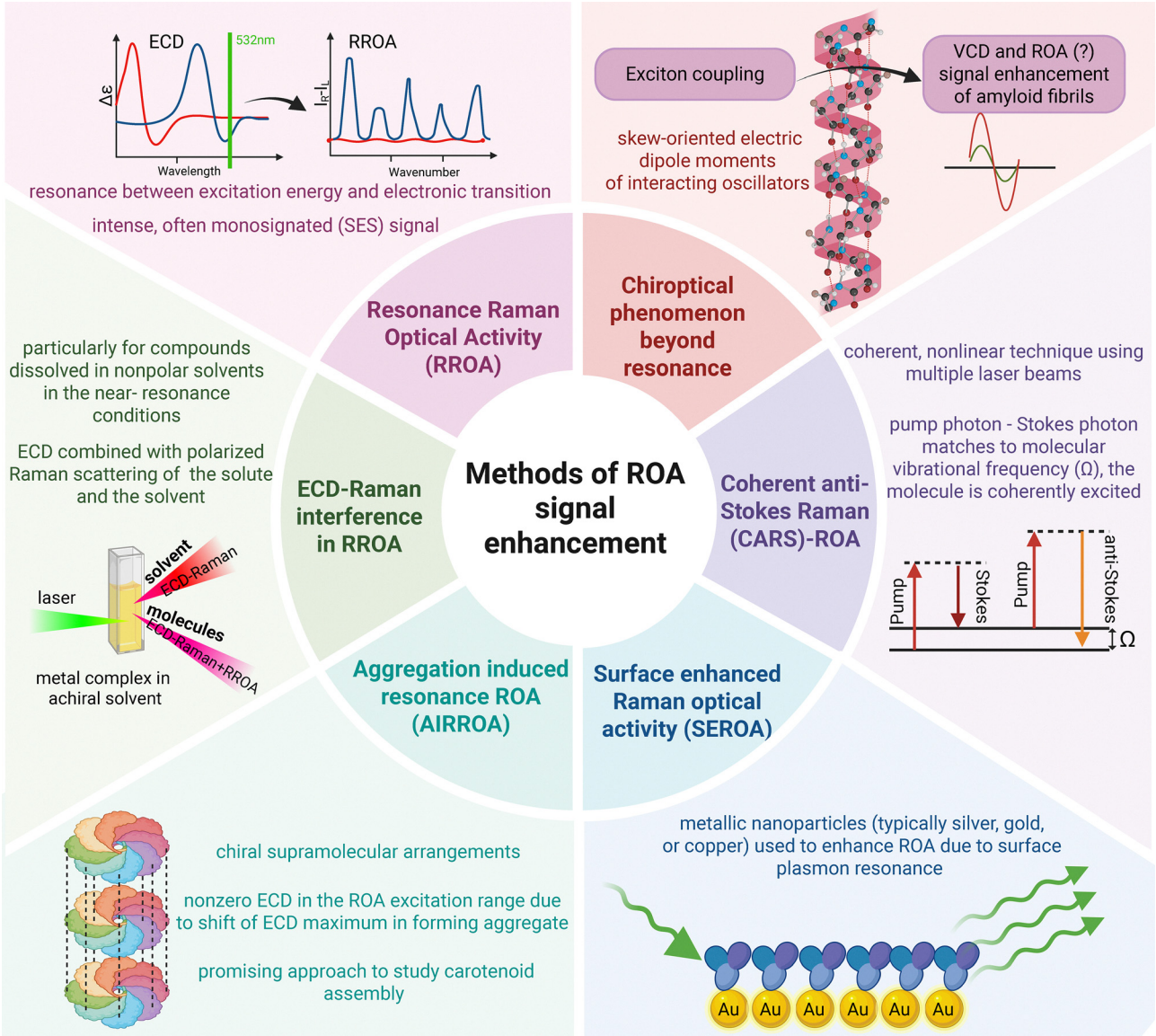

Fig. 1 Characteristics of techniques providing ROA signal enhancement.

via the following equation:[19]

$$\mathrm{CID} = -\frac{g}{2}$$

where CID is circular intensity difference, *i.e.*, the ratio of ROA-to-Raman intensity, and g is the dissymmetry factor, *i.e.*, the ratio of ECD to electronic absorption intensity. This equation shows that, for a given ROA transition to yield a nonzero RROA signal, the ECD must also be nonzero at the wavelength corresponding to that of the ROA transition.

SES-RROA has been measured for multiple compounds, including naproxen,[20] carbon nanotubes,[21] retinoids,[22–30] and carotenoid aggregates.† [31–38] Monosignated SES-RROA lacks the stereostructural sensitivity characteristic of conventional ROA (Fig. 2A), although it remains a convenient tool for studying the organization of biosupramolecular systems, aggregation, and related phenomena.[31,33–36] We discuss this more extensively in the section devoted to retinoids and carotenoid aggregates.

RROA can be also registered together with far from resonance ROA (FFROA), if the FFROA signal is sufficiently intense, as shown for metalloproteins from the transferrin family (Fig. 2C).[39] As the theory of RROA *via* two states is considerably more complex, we refer the interested reader to the excellent book by Nafie.[2] RROA spectra with the contribution from more than one electronic excited state have been registered for metal-containing systems[17,40] including myoglobin.[41] In agreement with theory, such RROA is bisignated, hence the sensitivity for the stereostructure is 'recovered' (compared to SES-RROA), as we have shown explicitly for vitamin B_{12} and its derivatives (Fig. 2B).[40]

† Being more exact, for aggregates resonance does not involve one electronic excited state, but multiple states due to different molecules. However, as the energy of these states is very similar, they can be approximately considered as a single excited state.

 This journal is © The Royal Society of Chemistry 2025

Open Access Article. Published on 02 2025. Downloaded on 06.02.2026 19:38:33.
This article is licensed under a Creative Commons Attribution 3.0 Unported Licence.

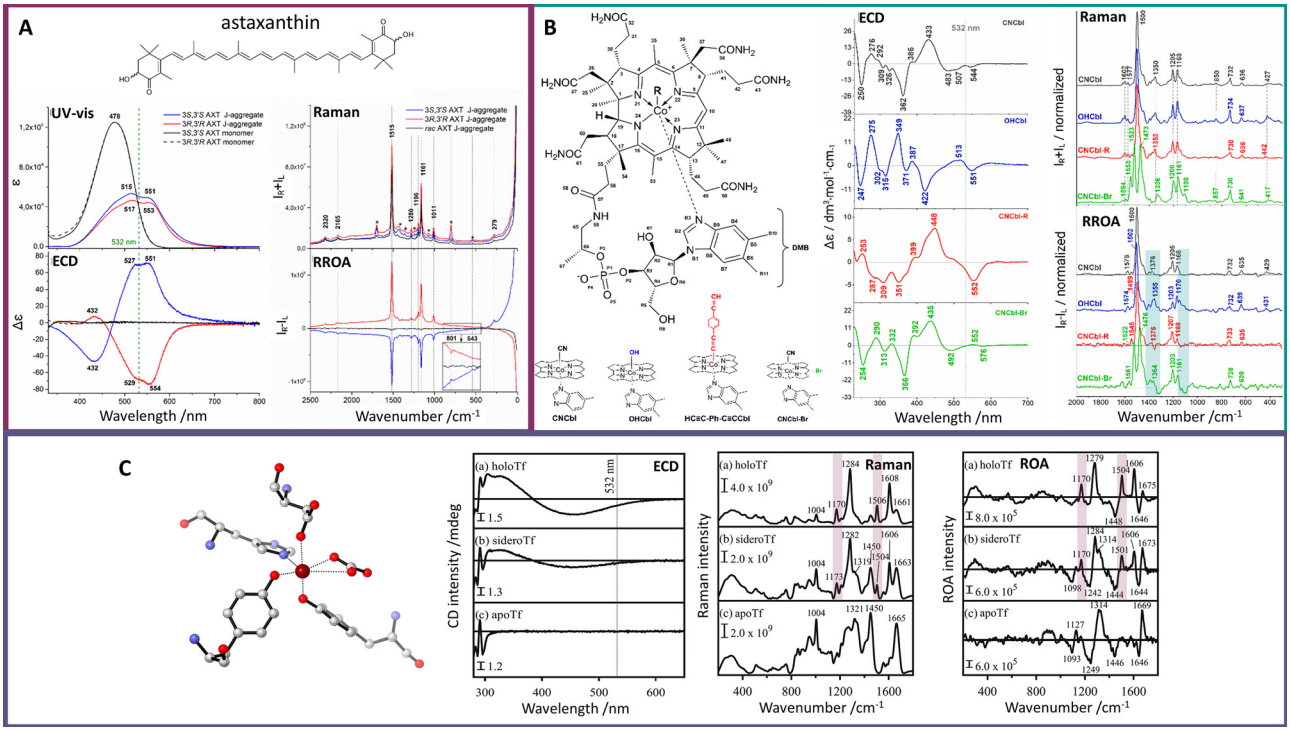

Fig. 2 Resonance ROA (RROA) *via* a single electronic state (A)†, multiple electronic states (B) and RROA registered together with FFROA (C). (A) The molecular structure of astaxanthin and electronic absorption (UV-vis), ECD, Raman and RROA spectra of 3*R*,3′*R*- and 3*S*,3′*S*-astaxanthin 3 : 7 water : acetone aggregates and monomers (red and blue, and black lines, respectively). Raman bands denoted with a star (*) are due to the solvent. RROA spectra of aggregates are monosignated (either positive or negative for 3*R*,3′*R* and 3*S*,3′*S* aggregates, respectively), with relative intensities as in the parent Raman spectra. Adapted with permission from ref. 38. Copyright 2016 American Chemical Society. (B) The molecular structure of vitamin B_{12} and its derivatives, and ECD, Raman and RROA spectra of cobalamins with different upper axial substituents: cyanocobalamin (R═CN), hydroxocobalamin (R═OH), 1,4-diethynylbenzenecobalamin (R═C≡C–Ph–C≡CH), and a cobalamin ring derivative [(C_{10})H═Br]. RROA spectra are bisignated (key regions denoted in green) and enable distinguishing vitamin B_{12} derivatives, in contrast to the parent Raman spectra. Adapted with permission from ref. 40. Copyright 2020 American Chemical Society. C Fe^{3+} binding pocket of the N-lobe of human serum transferrin (PDB id. 1N84), as well as ECD, Raman and ROA spectra of holo, sidero and apo transferrin, showing that ROA can simultaneously provide information on the metal binding pocket (RROA, key bands denoted in violet) as well as on the secondary structure of the protein (FFROA). Adapted with permission from ref. 39.

2.1.1. ECD-Raman (eCP-Raman) interference in RROA. Given that most commonly RROA has been measured using 532 nm excitation, the potential candidates for RROA are often metal complexes with electronic absorption in the visible range. Many of these compounds are nonpolar, hence not soluble in aqueous solution, which led to the discovery of a new phenomenon, currently called ECD-Raman or eCP-Raman. Between 2015 and 2020 ROA scientists, including researchers from our group, began noticing an unusual effect: the appearance of very intense bands from achiral solvents in 'RROA' spectra. Xu, Bouř, Kapitan and co-workers explained the origin of this effect,[42] which is especially relevant for nonpolar solvents in near-resonance conditions, where it can completely obscure the RROA signal.

ECD-Raman is related to ECD combined with polarized Raman scattering of both the solute and the solvent, occurring in the ROA cuvette together with the genuine RROA.[42–44] The magnitude of this effect can be estimated according to an empirical equation, which appears in several versions across the literature.[42,44,45] Below, we present the form reported by Xu, Bouř, and co-workers:[44]

$$\mathrm{CID} = \frac{\ln 10}{4} cL\Delta\varepsilon\left(\frac{\Delta\varepsilon'}{\Delta\varepsilon} + \mathrm{DOC}\right)$$

where $\Delta\varepsilon$ and $\Delta\varepsilon'$ denote ECD intensity (in L mol^{-1} cm^{-1}) for excitation and scattering, respectively, L is the optical path length (in cm^{-1}), c is the concentration of the solute (in mol L^{-1}), and DOC is the degree of circularity of either the solvent or the solute.

The polarized Raman scattering enters the equation *via* DOC, which for backscattering, is defined as the difference in the co-rotating Raman spectrum ($I_R^R - I_L^R$) minus the contra-rotating Raman spectrum ($I_R^R + I_L^R$) divided by their sum:[1,2]

$$\mathrm{DOC}(180°) = \frac{I_R^R - I_L^R}{I_R^R + I_L^R}$$

DOC pertains to polarizability changes during vibrational transitions of both the solute and the solvent and is significantly more pronounced in nonpolar solvents.[42,44,46] The discovery of the ECD-Raman effect sparked a discussion in the community about the possibility of measuring genuine RROA and cast doubt on the previously obtained RROA spectra. Nevertheless, recently, we have learned that this effect is important only in some specific cases and, even then, can be successfully eliminated.

2.1.2. When is ECD-Raman negligible and how to eliminate it? Although ECD-Raman can be considered a new form of

Open Access Article. Published on 02 2025. Downloaded on 06.02.2026 19:38:33.
This article is licensed under a Creative Commons Attribution 3.0 Unported Licence.

chiral spectroscopy,[43] and it can have analytical applications,[46] in most cases, it is a phenomenon that needs to be removed. Over time, it was established that the effect is not so significant in polar solvents (which generate low DOC values) or in systems under strong resonance conditions.[33] Even in problematic cases, such as nonpolar compounds (often metal complexes), dissolved in nonpolar solvents under near-resonance conditions, ECD-Raman can be minimized (using short path lengths,[45] low concentrations *etc.*) or eliminated using a correction factor.[47]

Recently, we also proposed a simple strategy for nearly complete elimination of the ECD-Raman effect for nonpolar metal complexes that are completely insoluble in water.[48] By encapsulating a nonpolar compound in micelles made of Pluronic F-127, we were able to measure RROA in aqueous solution, where the low DOC contribution decreases the ECD-Raman contribution.[48] The above mentioned considerations show that although the ECD-Raman effect is important under some circumstances (near resonance, nonpolar compounds, hence nonpolar solvents), it can be minimized even under these conditions, enabling measurements of genuine RROA. Fortunately, the most desirable solvent for ROA—water—does not typically generate a significant ECD-Raman signal, therefore enabling analysis of biological systems. Two groups of such systems that provide RROA and are relatively well-explored—retinoid–protein complexes and carotenoid aggregates—will be discussed below.

2.1.3. RROA of chromophores in protein environment. Photoreceptor proteins containing covalently or non-covalently bound light-absorbing chromophores represent particularly interesting supramolecular systems that have been successfully studied using ROA. In such systems, the protein environment can cause deformation, leading to distortion of an achiral chromophore into a chiral one (Fig. 3). Extensive research in this area was conducted by Unno, Fujisawa, and co-workers, who employed ROA to precisely determine the structure of chromophores in several functional proteins using a non-commercial setup with near-infrared excitation (785 nm) to measure pre-resonance ROA.[24] Obtained ROA spectra showed distinct spectral features, including enhanced chromophore bands and non-resonant protein bands. One of the studied systems was photoactive yellow protein from *Salinibacter ruber*, comprising a *p*-coumaric chromophore in the protein active site. ROA spectra were recorded for this protein under both resonance (532 nm laser) and pre-resonance (785 nm laser) conditions.[25] ROA spectra obtained with 532 nm excitation were dominated by negative bands attributed to the chromophore, with the exception of the non-resonant positive protein band at 1667 cm^{-1} (amide I). Results indicated resonance enhancement of chromophore vibrations and were in good agreement with RROA theory. At 785 nm, chromophore band remained enhanced, and it was thus possible to selectively observe the chromophore with minor contribution of the protein to the spectra.[25] Similar experiments employing pre-resonance ROA at 785 nm were also conducted for photoactive yellow protein from phototrophic bacterium *Halorhodospira halophila*, containing 4-hydroxycinnamyl chromophore.[30] Pre-resonance ROA enhancement was explored as well to study the conformation of the carotenoid chromophore (3′-hydroxyechinenone) in the active site of orange carotenoid protein (OCP) and its structural changes during photoconversion from the orange inactive state (OCP^O) to the red active state (OCP^R).[22] When excited at 785 nm, both forms exhibited distinct ROA spectra arising from different chromophore conformations. In the observed ROA, bands were predominantly negative and opposite in sign to those of ECD. The ROA-to-Raman intensity ratio deviated from the values predicted by the SES theory, indicating that the measured ROA involved contributions from more than one electronic state.[22]

Near-infrared ROA spectroscopy was also used to investigate microbial rhodopsins.[23,27–29] In one of the examples, an all-*trans* retinal protonated Schiff base chromophore in two microbial rhodopsins (proton pump *Gloeobacter rhodopsin*—GR; sodium-ion-pumping rhodopsin—NaR) was studied.[27] As the chromophore was distorted in opposite directions in those two proteins, ROA spectra showed an inverted sign for the studied systems, *i.e.*, GR spectrum was monosignated and positive, whereas that of NaR exhibited only negative bands.[27] Realization of the experiment provided the first experimental confirmation that the direction of the retinal chromophore's twist determines the sign of the ROA signal. Similar results were obtained for the chloride-pumping rhodopsin from *Flavobacterium*; however, for

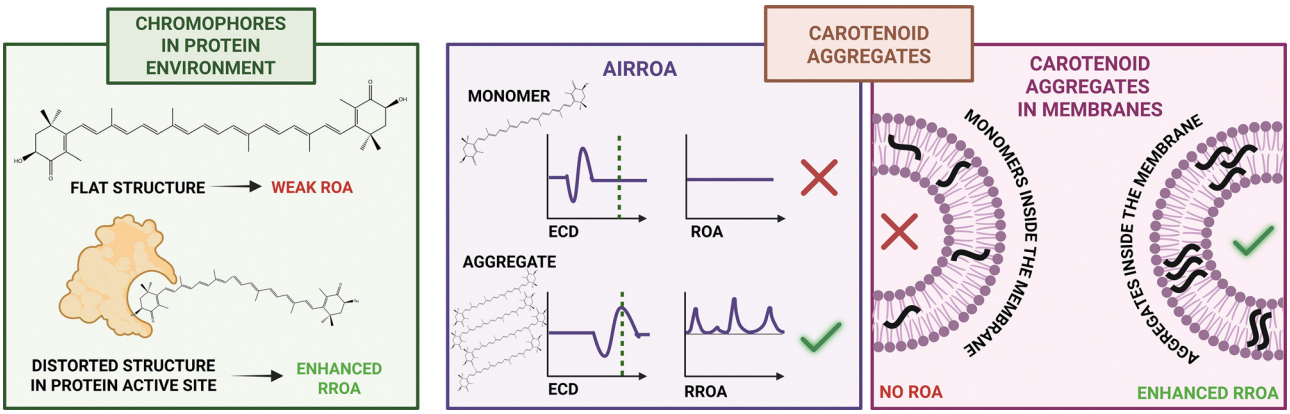

Fig. 3 Examples of supramolecular systems exhibiting ROA signal enhancement *via* electronic resonance.

Open Access Article. Published on 02 2025. Downloaded on 06.02.2026 19:38:33.
This article is licensed under a Creative Commons Attribution 3.0 Unported Licence.

halorhodopsin from the cyanobacterium *Mastigocladopsis repens*, the ROA spectrum was bisignated, which was attributed to the presence of the chromophore in two distinct conformations with the opposite twist.[29]

Although in the aforementioned studies ROA features of rhodopsins could be well explained from protein crystal structure, the case of sensory rhodopsin II showed that crystal structure may contradict the ROA spectra obtained in solution.[28]

Ultimately, these observations emphasize the unique capabilities of ROA to selectively observe chromophores in a protein's active site due to pre-resonance enhancement and to gather detailed information about cofactor's structure, especially when aided by quantum mechanics/molecular mechanics calculations.

2.1.4. RROA of carotenoid aggregates. As mentioned in the previous section, ROA spectroscopy proved to be an efficient tool for studying carotenoids, or, more precisely, their aggregates. The phenomenon where ROA resonance is 'turned on' as a result of aggregation is known as aggregation-induced resonance ROA (AIRROA; Fig. 3).[38] Monomeric carotenoids by themselves do not exhibit ROA signals (neither normal nor resonant) plausibly due to the substantial distance between the chiral centres, typically located at terminal part of the molecule, and the chromophore within the carotenoids' structure. However, under certain conditions, among others in two solvents of different polarity, carotenoids are able to form aggregates, including assemblies of so-called *J*- or *H*2-type, where polyene chains are stacked next to one another. Organization into chiral supramolecular arrangements of this type results in the bathochromic shift of the absorption band due to the $\pi \rightarrow \pi^*$ transition, leading to the appearance of the strong ECD couplet. Consequently, if the energy of the electronic transition is close to the energy of the excitation laser, a strong ROA resonance is 'switched on.'[38] First, AIRROA spectra were reported by us for astaxanthin (AXT) *J*-type aggregates.[38] Carotenoid aggregates exhibited a monosignated spectra that was opposite in sign to the corresponding ECD signal at 532 nm (excitation wavelength; Fig. 2). Moreover, two measured AXT enantiomers, (3*R*,3′*R*) and (3*S*,3′*S*), generated 'mirror image' spectra. RROA was obtained for AXT concentration of *ca.* $1 \cdot 10^{-5}$ M, which is notably lower than for typical ROA experiments. Despite that, spectra were significantly enhanced, with ROA/Raman ratio up to 10^{-2} – an order of magnitude more compared to values reported for RROA of naproxen[20] (which was the first experimentally measured RROA spectra). Moreover, the exceptional enhancement allowed the observation of overtones and combinatorial bands, which was unprecedented for ROA spectroscopy.[38] Following the success of astaxanthin, we confirmed the AIRROA effect for different types of AXT aggregates (*J* and *H*2),[49] as well as for other carotenoids, including zeaxanthin,[32] lutein, and lutein derivatives.[50] Importantly, the RROA of carotenoid aggregates exhibited monosignated ROA spectra, in accordance with SES theory.[1,19] However, the observed ROA-to-Raman bands ratios deviate from the predictions of SES, exceeding the theoretical values. Such contradiction may occur due to the added enhancement coming from supramolecular aggregation.

Discovery of the AIRROA phenomenon opened the door for the investigation of more complex systems containing carotenoid aggregates. One such system was analyzed in our study of carotenoid microcrystals extracted from carrot root cells.[31] These microcrystals mainly comprise achiral β-carotene with only a minor (~5%) contribution of chiral carotenoids (α-carotene, astaxanthin), and yet, they exhibit strong ECD and RROA signals. ROA-based comparison with model systems of varied mixed non-chiral and chiral carotenoid aggregates showed that the signal enhancement originates from the 'sergeant-and-soldier'-like chirality induction (Fig. 3), evidencing that this phenomenon may transpire spontaneously in nature.[31] It was also reported that canthaxanthin, a non-chiral carotenoid, can form chiral supramolecular assemblies triggered by asymmetric polysaccharides.[51]

Recently, we also investigated the aggregation of carotenoids (α-carotene, fucoxanthin and zeaxanthin) in model membranes (dipalmitoylphosphatidylcholine (DPPC) liposomes).[33] Due to their hydrophobic nature, carotenoids in living organisms are found either complexed with proteins or incorporated in membranes, where they strongly influence membrane characteristics, such as mechanical strength, fluidity, and permeability. Because of the significantly enhanced RROA signal of carotenoid assemblies, it was possible to use this technique as a tool for selectively studying aggregation in a bilayer in the presence of monomers, which is not possible with traditional Raman spectroscopy. We demonstrated that orientation of carotenoid assemblies in membranes and the monomer structures within the assemblies directly influence the stability of aggregates in the model bilayer.[33] Taking advantage of ROA selectivity toward aggregates, we also monitored encapsulation of enantiopure (3*S*,3′*S*)-AXT in Pluronic F-127 nanoparticles providing detailed information about the carotenoid assemblies inside the micelles.[36]

The AIRROA phenomenon also proved to be useful in studies of carotenoid–protein complexes, where we used RROA as an auxiliary method to characterize the structure of the enantiopure either (3*S*,3′*S*)- or (3*R*,3′*R*)-AXT bound to bovine serum albumin (BSA).[34,35]

Overall, the body of work so far on ROA of carotenoid aggregates demonstrates the unique potential of ROA spectroscopy, and more precisely, the resonance enhancement of ROA, for studying natural biological systems with amplified chirality, both in model assemblies and complex biosupramolecular systems.

2.2. Surface-enhanced Raman optical activity

An effective way to reduce sampling requirements and expand the range of ROA applications is by combining it with plasmon resonance enhancement. Drawing inspiration from surface-enhanced Raman spectroscopy (SERS)—which relies on the enhancement of Raman scattering by metal nanostructures[52]—this approach has led to the development of a novel technique known as surface-enhanced Raman optical activity (SEROA). SEROA applies the same principle as SERS to study chiral molecules, analyzing their optical activity in response to polarized light.[53]

Open Access Article. Published on 02 2025. Downloaded on 06.02.2026 19:38:33.
This article is licensed under a Creative Commons Attribution 3.0 Unported Licence.

One of the main challenges of SEROA lies in its sensitivity to the local environment and the fluctuating conditions experienced by chiral molecules on a SERS surface. Hot spots, which vary over time, complicate the acquisition of stable SEROA spectra and hinder the observation of mirror-image signals for enantiomers.[54]

Initial studies reported SEROA spectra for resonant metalloproteins, such as cytochrome *c*, myoglobin, and the myoglobin–azide complex, where the resonant parts were shielded from the metal surface by non-resonant protein structures.[55,56] Additionally, a successful SEROA measurement was achieved for the non-resonant pentapeptide met-enkephalin in silver colloid solutions.[57] Although good signal-to-noise ratios were obtained, the lack of enantiomeric pairs prevented full validation of the chiroptical signals.

Surface-enhanced resonant ROA (SERROA) signals were later observed for adenine adsorbed on silver colloids, attributed to adsorption-induced chirality.[58] Building on this, significant progress was made by using gel-forming polyacrylic acid linkers to position D- and L-ribose near metal surfaces without direct contact. This stabilization allowed clear observation of mirror-image SERROA spectra,[59] marking an important step toward reliable chiral sensing.

Further advancements were introduced by Das *et al.*,[60] who developed new strategies to enhance sensitivity and reproducibility of SEROA measurements. One approach employed the sergeant-and-soldiers effect, where small amounts of chiral analytes induced chirality in linker molecules adsorbed on silver colloids.[60] A more direct method followed, with silver nanoparticles synthesized in the presence of chiral analytes, yielding bisignate SEROA spectra and enabling simultaneous detection of analyte and reporter bands.[61]

A novel breakthrough involved the remote transfer of chirality using plasmonic nanomaterials. Nanotags, consisting of silver nanoparticles coated with benzotriazole dye and encased in a silica shell, remained achiral until binding with chiral molecules, such as L- and D-ribose or L- and D-tryptophan. Upon binding, mirror-image SERROA spectra emerged. Computational simulations confirmed that chirality transfer occurred *via* symmetry breaking induced by electromagnetic interactions near the nanoparticles, without direct chemical bonding.[62]

Thanks to these advancements, SEROA may offer powerful capabilities across a range of applications, including drug development, probing molecular organization, ligand binding, and self-assembly processes on surfaces.

2.3. Coherent anti-Stokes ROA (CARS-ROA)

Another approach to increase the intensity of ROA is coherent anti-Stokes Raman optical activity (CARS-ROA), a chiral equivalent of coherent anti-Stokes Raman spectroscopy. In CARS, two synchronized laser ('pump' and 'Stokes') pulses are used, frequency tuned to a vibrational mode to generate anti-Stokes scattering.[63] CARS scattering typically generates a large, intense signal that can obscure the weaker ROA signal, making it difficult to isolate the chiral information.[64] To overcome this challenge, a heterodyne-detected, polarization-resolved technique is employed, where crossed polarizers suppress the dominant in-phase CARS signal, allowing the much weaker out-of-phase ROA signal to be selectively detected.[65] A pioneering experimental demonstration of heterodyne-detected CARS-ROA with a pulsed laser source was carried out using a pure chiral liquid: (−)-β-pinene.[65] It was shown that for liquid (−)-β-pinene, the CARS-ROA signal-to-achiral CARS background ratio is approximately two orders of magnitude greater than the ratio observed in spontaneous ROA relative to Raman scattering.[63,65,66] Subsequently, it was shown that CARS-ROA spectra of chiral molecules, namely (*S*/*R*)-MOM-BINOLs, can be experimentally obtained even in the presence of achiral solvent molecules.[67] CARS-ROA offers significant advantages over conventional spontaneous spectroscopy in terms of analytical sensitivity and acquisition times, in particular the measurement time from hours to less than a minute. It could be particularly beneficial for studying low-concentration or fluorescent samples, which are challenging to analyze using traditional ROA techniques. In theory, the CARS-ROA technique could be also used for investigating dynamic processes on ultrafast timescales. However, the limited number of CARS-ROA measurements and experimental setups makes it difficult to assess its further development and practical applicability.

3. Chiroptical phenomenon beyond resonance: amyloid fibrils

As this work primarily discusses the enhancement of the ROA signal in amyloid fibrils, the following sections will delve into the remarkable structural features of these materials that generate an exciton coupling-enhanced VCD response, strongly linked to long-range supramolecular chirality.[68] Furthermore, emerging evidence suggests that ROA spectra of amyloid fibers also display distinct enhancement effects, highlighting a promising and potentially significant direction for future research.

3.1. The essence of amyloid fibril structure

Amyloid fibrils are commonly associated with neurodegenerative diseases, such as Alzheimer's and Parkinson's. However, due to their unique properties like high stiffness, biodegradability, and large surface-to-volume ratio, they are gaining attention as advanced nanomaterials.[69,70] One of their most remarkable features is structural polymorphism—meaning they can adopt various forms depending on aggregation conditions. Identifying and characterizing these polymorphs is essential to understanding how the structure relates to the material properties. Traditionally, amyloid fibrils were thought to conform to the canonical model, which describes amyloid fibrils as cross-β structures with stacked β-sheets; however, recent studies reveal the existence of fibrils with alternative secondary structures, such as α- or polyproline II-helices.[71,72] Amyloid fibrils, regardless of their secondary structure, can adopt various morphologies, such as nanotubes, twisted ribbons, or helical ribbons.[73] This structural diversity contributes to differences in thermodynamic stability and material

 This journal is © The Royal Society of Chemistry 2025

Open Access Article. Published on 02 2025. Downloaded on 06.02.2026 19:38:33.
This article is licensed under a Creative Commons Attribution 3.0 Unported Licence.

properties. Chirality is another key feature of fibrils and may appear at different structural levels.[68,74] As fibrils are composed of proteins made from L-amino acids, it was initially assumed that chirality of the protofilaments and the overall handedness at the mesoscopic level would follow the same pattern. However, numerous studies have shown that fibrils can adopt both right- and left-handed twisted structures, often appearing as mirror images of each other.[75–77] This challenges the assumption that their handedness would be uniform and suggests a more complex structural organization. Interestingly, not all fibril structures are permanently stable. Under certain conditions, they may undergo reversible transformations.[78,79] The stability of β-sheet fibrils comes from strong hydrogen bonds, while α-helical forms are held together by weaker hydrophobic interactions, making them more prone to rearrangement.[79] A detailed understanding of the structural variability, chirality, and stability of amyloid fibrils is crucial for developing new applications in biotechnology, materials science, and also for advancing the treatment of neurodegenerative diseases.

3.2. VOA enhancement by exciton coupling

In many cases, particularly in large molecular assemblies, supramolecular chirality plays a dominant role in shaping VOA spectra. For example, in proteins, secondary structural elements such as α-helices or β-sheets strongly influence the appearance of VCD and ROA signatures.[80–82] However, it particularly affects the spectra of amyloid fibrils. In this case, the enhancement of the amide I signal arises from excitonic coupling between C═O vibrational dipoles that are arranged in a skewed spatial geometry. This interaction leads to the formation of a couplet, characterized by two signals of opposite sign, which reflects the chiral organization of the system.[1,83,84] The strong VCD signals observed in amyloid fibrils are linked not only to their macroscopic twist but more specifically to the chirality at the protofilament level. VCD has proven to be a powerful tool for identifying protofilament handedness, as supported by quantum-chemical calculations showing that the sign of the amide I couplet reflects the twist direction between stacked β-sheet structures.[85,86] Opposite couplet signs indicate reversed protofilament chirality.[68,76,86] Interestingly, enhanced VCD is also seen in fibrils lacking β-sheets, such as those formed from zwitterionic tripeptides adopting distorted or inverse polyproline II-like conformations.[87,88] The VCD intensity may also be influenced by strand orientation (parallel or antiparallel). As fibril VCD signals are typically two orders of magnitude stronger than those of native proteins, VCD offers unique sensitivity for fibril characterization.[89,90]

3.3. ROA *vs.* VCD and ECD

VCD and ROA share many similarities, as both belong to the same family of VOA techniques and originate from the same vibrational force field and normal mode frequencies.[64] They depend on the same molecular forces acting within a molecule and also consider its conformation, absolute configuration, and enantiomeric excess, thereby providing equivalent molecular-level information. However, while VCD focuses more on the internal structure of the molecule, ROA is also more sensitive to the molecule's surface and its interactions with the surrounding environment. Our previous study has demonstrated that ROA does not exhibit the same sensitivity to the supramolecular chirality of amyloid fibrils as observed in VCD (Fig. 4).[18] Although both ROA and VCD signals can exhibit substantial enhancements—for mature fibrils, up to one or two orders of magnitude—they do not respond with equal sensitivity to the progressive stages of amyloid supramolecular chirality (Fig. 5A).[18,91]

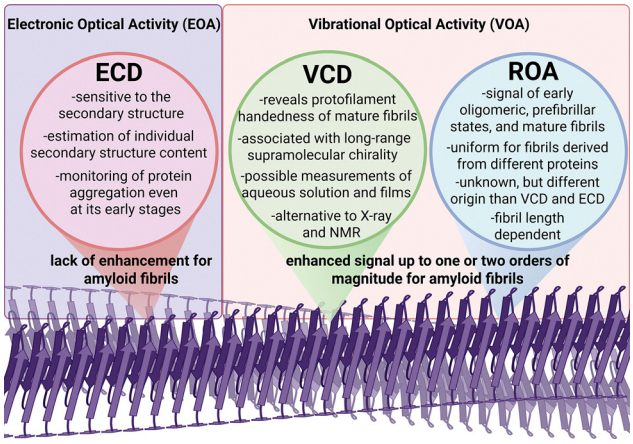

Fig. 4 Comparison of information provided by chiroptical spectroscopies for amyloid fibrils.

This suggests that each technique probes distinct aspects or hierarchical levels of chiral organization within fibril structures. ROA of mature fibrils is uniform for fibrils of three different proteins and is considerably more intense and dissimilar compared to ROA of native proteins (Fig. 5B).[18]

In general, ROA is inherently a more localized spectroscopic technique, lacking the capacity for long-range through-space coupling mechanisms that contribute to the strong VCD responses in vibrational bands such as the amide I (the carbonyl stretching vibration).[18,64] Furthermore, ROA has demonstrated potential in characterizing early oligomeric and prefibrillar states, thereby offering valuable insights into the initial stages of amyloid formation.[18,71,92,93] For amyloid fibrils, in addition to the characteristic amide I band, the ROA spectrum also exhibits other, less intense bands in the 1500–600 cm^{-1} region, which may help in structural characterization of these structures. The discrepancy between these methods may also stem from enhanced background scattering caused by fibrils approaching the dimensions of the visible wavelengths used in ROA and Raman spectroscopy, which can obscure the chiral signal. Additionally, measurements may be complicated by the fact that amyloid fibril samples are often heterogeneous and may simultaneously contain structures with varying chirality and morphology.[94,95]

Nevertheless, one of the main strengths of ROA spectroscopy lies in its applicability to measurements in aqueous solutions, which positions ROA as a potentially preferred tool in fibril studies, as VCD measurements in water are significantly more problematic (although possible for fibrils) and cover a narrower

Open Access Article. Published on 02 2025. Downloaded on 06.02.2026 19:38:33.
This article is licensed under a Creative Commons Attribution 3.0 Unported Licence.

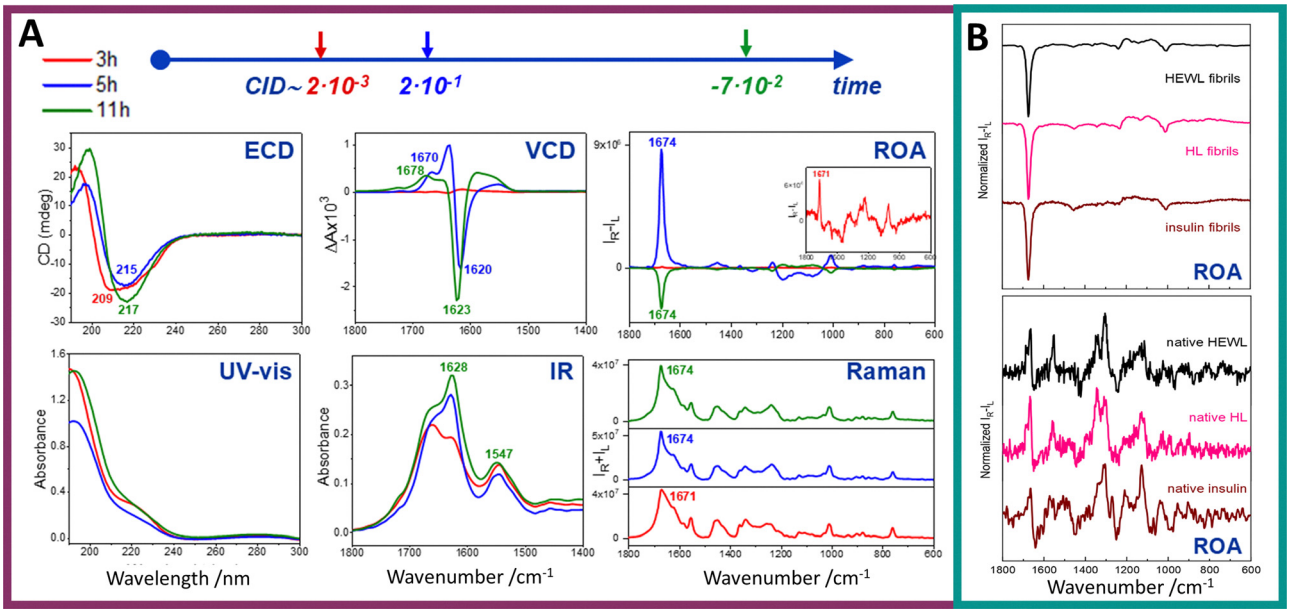

Fig. 5 Exceptionally enhanced ROA signal of amyloid fibrils. (A) Electronic absorption, ECD, IR, VCD, Raman and ROA spectra of hen egg white lysozyme (HEWL) prefibrillar states and fibrils obtained after 3, 5 and 11 h of incubation (red, blue and green lines, respectively). HEWL protofibrils/fibrils were formed *via* incubation at 60 °C of aqueous HEWL solution of an initial concentration of 60 mg mL^{-1} at pH 2.0 with agitation at 1400 rpm. Significantly enhanced ROA signal appears amid fibril formation. At shorter incubation time (5 h) a positive ROA signal is observed, while at longer incubation time (11 h) the signal's sign changes to negative. (B) Comparison of ROA spectra of amyloid fibrils obtained from different proteins shows the recurring ROA pattern (upper panel). Spectra recorded for fibrils from HEWL (black line), human lysozyme (HL, pink line), and insulin (dark red line). Respective ROA spectra of native proteins (bottom panel). While clear differences are visible for spectra of different proteins in their native state, when amyloid fibrils are formed, obtained spectra exhibit the same characteristics. Reproduced from ref. 18 with permission from the Royal Society of Chemistry.

range of wavenumbers—a factor particularly important given that amyloid fibrils typically form and exist in aqueous environments.

ECD is particularly sensitive to the secondary structure of proteins,[96] providing only information about rearrangements during protein aggregation and oligomerization. Given that the ECD signal refers to the secondary structure and not the higher levels of chiral organization, ECD lacks this exceptional sensitivity to amyloid fibril formation, characteristic for VCD and, to an even greater extent, ROA.

4. Perspectives and outlook

ROA has truly reached middle age at 50 years, as we recently concluded in a summary of up-to-date advances in ROA instrumentation and reflections on its future.[97] However, it is true that ROA is still perceived as an auxiliary technique compared not only with infrared and Raman spectroscopies but even with VCD, which is a counterpart of ROA. One of the reasons behind it is the low analytical sensitivity of ROA, although this feature is also shared by VCD. Others are the complexity of ROA instrumentation and susceptibility of ROA to artefacts. Despite this, among chiroptical techniques, ROA remains the method with the greatest potential for studying stereostructures of biological molecules and supramolecules. Its 'vibrational' sensitivity, provides local and well-defined molecular structural information (surpassing ECD), along with the ability to study aqueous solutions and access the low-energy region of the vibrational spectrum (surpassing VCD).

The relatively simple solution that enables the elimination (at least some) of the problematic ROA issues is the enhancement of ROA signal. It is therefore not surprising that there is a quest for both methods of signal enhancement (hence development of RROA, SERROA and CARS-ROA) and systems that provide intense ('enhanced') ROA.

Among the latter, amyloid fibrils provide rather unique ROA as they generate not only the most intense ROA observed up to now (as illustrated by CIDs up to 10^{-1}; Fig. 5) but are the only systems that provide such intense ROA without resonance enhancement. Clearly this exceptional sensitivity of ROA to amyloid fibrils opens new perspectives for their chiroptical studies (as elaborated below). However, before this method is used in biomedical research of fibrils, we need to answer some essential questions related to the interpretation of their ROA, of which the most important are discussed below. Some ideas for further studies that could be helpful in answering these questions are also given (Fig. 6).

4.1. What is the origin of the sensitivity of ROA to amyloid fibrils?

Here, we emphasize that (both intense) ROA and VCD signals of amyloid fibrils appear at different time points along the protein aggregation pathway and are not directly related (Fig. 5).[18] This clearly indicates that the origin of the intense ROA signal in

Open Access Article. Published on 02 2025. Downloaded on 06.02.2026 19:38:33.
This article is licensed under a Creative Commons Attribution 3.0 Unported Licence.

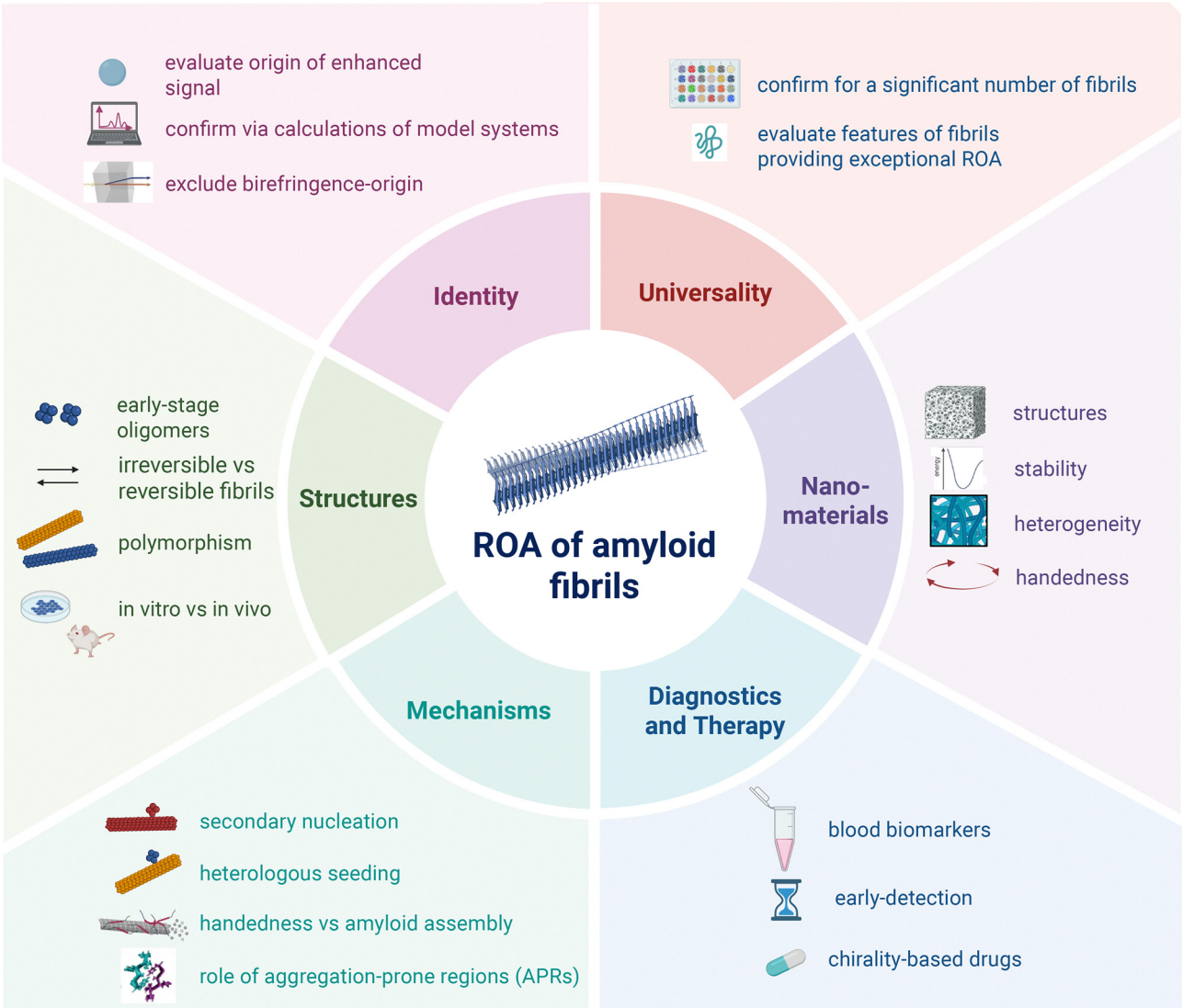

Fig. 6 Further steps necessary to develop ROA of amyloid fibrils and its potential applications.

fibrils is not merely excitonic coupling due to the protofilament twist, as is currently assumed for the origin of VCD.[68,75,76,91,98] However, it is clear that the ROA intensity is driven by long-range interactions, as the signal diminishes upon fibril sonication, which causes structural fragmentation.[18] Nonetheless, the first step for correct interpretation of ROA of fibrils is to fully rule out the possibility that it is derived from sample birefringence. Furthermore, a direct correlation of the fibril size (length, thickness) with the ROA intensity could be helpful. A separate aspect is computational modelling of amyloid fibrils and predicting their ROA that could directly provide information regarding the 'enhancement' origin. While we acknowledge that we are not practitioners in this field, we believe that, at present, it may be beyond the state of the art to computationally capture the architectural complexity of amyloid fibrils and predict their ROA spectra in a way that meaningfully supports experimental studies. Therefore, for now, we have to concentrate on experimental approaches.

4.2. What types of fibrils generate intense ROA?

We have shown that not all types of fibrils generate intense ROA. The essential issue is, therefore, to define structural and morphological features of fibrils that provide the 'enhanced' signal. Such studies would require analyzing a significant number of fibril systems, preferentially obtained from different proteins and also differing by structure and morphology, using high-spatial-resolution microscopic methods (TEM, SEM, AFM, *etc.*) coupled with ROA and conveniently also VCD and ECD. Such an approach could not only provide data regarding structure-signal correspondence but also address another essential issue, *i.e.*, if the intense ROA signal is a typical feature of amyloid fibrils, or if there are only some unique types of amyloid architectures that provide such 'enhanced' signals.

4.3. What is the relation between ROA sign and fibril handedness?

In the case of using handedness-sensitive methods, such as SEM, AFM or (in some cases) cryo-EM, such analysis could also

Open Access Article. Published on 02 2025. Downloaded on 06.02.2026 19:38:33.
This article is licensed under a Creative Commons Attribution 3.0 Unported Licence.

shed light on the relation between ROA signal and the handedness of fibril structures at different levels of their organization. While performing such analysis, one also has to keep in mind that structures in solution (analyzed with ROA) might not be 1 : 1 identical to those observed *via* SEM and AFM, where sample preparation requires solvent evaporation during sample deposition on the substrate. Additionally, the high-resolution microscopic methods, while invaluable, do not provide information about the 'statistical' chirality in the bulk sample.

4.4. Perspectives of ROA applications in biomedical studies and for nanomaterial characterization

If we confirm that intense ROA is a characteristic (rather than exceptional) feature of fibril architectures and if the origin of the signal is clarified, it opens the door for application of ROA of fibrils in biomedical research.

One of the essential issues to analyze is the relation between the structure, handedness and toxicity of the fibril structures. Cryo-EM studies have demonstrated that the structures of amyloid fibrils are more diverse and intricate than previously expected,[99,100] and it is known that different fibril architectures may differ considerably in cytotoxicity.[101] Intriguingly, *ex vivo* fibril structures, solved using cryo-EM, are different from the structures that have been observed either *in vitro* or in patient-derived samples *via* seeding.[102,103] In this context, it would be very important to correlate (if possible) the structural features and handedness of amyloid fibrils with their toxicity. This should be done on a significant population of fibril structures, particularly those obtained *ex vivo*. ROA (and VCD) are well-suited for such studies, in contrast to techniques like cryo-EM, which, although capable of providing structures with atomic resolution require individual, well-separated, and sufficiently concentrated fibrils (which is why cryo-EM often relies on *in vitro*-derived samples prepared from *ex vivo* material).[104]

From the point of view of amyloidosis prevention, it is also necessary to understand what structural features (if such can be determined) determine the irreversibility *versus* reversibility of formation of proteinaceous aggregates. Moreover, due to habitual coexistence of two or more different types of protein aggregates in various neurodegenerative diseases,[105] it is also essential to comprehend mechanisms of heterologous seeding processes.

Last, but not least, the distinct and very intense ROA signal of amyloid fibrils, very different from the signal of the native protein, makes it plausible to follow the aggregation processes and potentially could be used for diagnostic purposes.

A detailed understanding of fibril polymorphism, its reversibility, and the potential of various polymorphs to undergo structural changes after formation is also essential for the controlled synthesis of fibril nanomaterials with designed architectures and long-term stability.

5. Conclusions

The majority of methods developed for enhancing ROA signals utilize resonance—either in a straightforward manner, by coupling of the laser energy with the energy of the electronic state (RROA) or through more complex approaches, such as coherent excitation of two laser beams resonant with molecular vibrations (CARS-ROA), enhancement *via* metal nanoparticles (SE(R)ROA) or aggregation-induced RROA (AIRROA). Using these techniques, a variety of different samples have been studied with improved analytical sensitivity.

Amyloid fibrils are unique systems that exhibit exceptionally intense ROA signals, even in the absence of resonance enhancement. Although the remarkable ROA response of amyloid fibrils has only recently been observed, and some insights have been established, many issues remain unresolved. We have shown that during protein aggregation, ROA appears earlier (also more intense) than VCD. While ROA is plausibly related to excitonic coupling, it reflects a different level of handedness than VCD. A critical next step is to determine the origin of the signal and whether it is a universal characteristic of majority of fibril structures.

If the origin of the ROA signal is explained and its universality is confirmed, ROA could become a powerful tool in the study of amyloid fibrils. This includes applications in characterizing fibril-based nanomaterials, and, above all, in biological and medical research, particularly relevant to neurodegenerative diseases, which are increasingly common in aging societies. ROA (coupled with VCD, ECD and microscopic methods) could shed light on such fundamental subjects as structure of early-stage oligomers, irreversibility *versus* reversibility of different stages of the aggregation process, relation between fibril structure/handedness and toxicity, mechanism of heterologous seeding *etc.* Additionally, given the distinct differences between spectra of native proteins and fibrils, ROA could be used in diagnostic contexts.

Although the future trajectory of ROA studies of fibrils cannot yet be predicted, the ROA signal of fibrils is undoubtedly a very intriguing phenomenon, both conceptually, as well as in light of potential practical applications of this method in fibril studies.

Author contributions

Conceptualization – A. Ko., A. W., A. Ka., supervision – A. Ka., writing – original draft – A. Ko., A. W., A. Ka., writing – review & editing – A. Ko., A. W., A. Ka.

Conflicts of interest

There are no conflicts to declare.

Data availability

As the article is a feature article, the data supporting this article can be found in the original articles, discussing the topic.

 This journal is © The Royal Society of Chemistry 2025

Open Access Article. Published on 02 2025. Downloaded on 06.02.2026 19:38:33.
This article is licensed under a Creative Commons Attribution 3.0 Unported Licence.

Acknowledgements

This publication has been funded by the National Science Centre, Poland: OPUS 25 (project no. 2023/49/B/ST4/01785 to A.K.). The open-access publication of this article has been supported by a grant from the Faculty of Chemistry under the Strategic Programme Excellence Initiative at Jagiellonian University. TOC and Fig. 1, 3, 4 and 6 were created in **https://BioRender.com**.

Notes and references

1 L. D. Barron, *Molecular Light Scattering and Optical Activity*, Cambridge University Press, Cambridge, 2nd edn, 2004.
2 L. A. Nafie, *Vibrational Optical Activity: Principles and Applications*, 2011.
3 F. M. S. Junior and J. M. B. Junior, *Chiral Separations and Stereochemical Elucidation*, 2023, pp. 551–591, DOI: **10.1002/9781119802280.ch14**.
4 P. Michal, J. Hudecová, R. Čelechovský, M. Vůjtek, M. Dudka and J. Kapitán, *Symmetry*, 2022, **14**, 990.
5 P. L. Polavarapu, *Molecules*, 2016, **21**, 1056.
6 L. D. Barron and L. Hecht, *Comprehensive Chiroptical Spectroscopy*, 2012, pp. 759–793, DOI: **10.1002/9781118120392.ch23**.
7 P. W. Atkins and L. D. Barron, *Mol. Phys.*, 1969, **16**, 453–466.
8 L. D. Barron and A. D. Buckingham, *Mol. Phys.*, 1971, **20**, 1111–1119.
9 L. D. Barron, M. P. Bogaard and A. D. Buckingham, *Nature*, 1973, **241**, 113–114.
10 W. Hug and G. Hangartner, *J. Raman Spectrosc.*, 1999, **30**, 841–852.
11 L. D. Barron, A. R. Gargaro and Z. Q. Wen, *Carbohydr. Res.*, 1991, **210**, 39–49.
12 M. Dudek, G. Zajac, E. Szafraniec, E. Wiercigroch, S. Tott, K. Malek, A. Kaczor and M. Baranska, *Spectrochim. Acta, Part A*, 2019, **206**, 597–612.
13 L. D. Barron, E. W. Blanch, I. H. McColl, C. D. Syme, L. Hecht and K. Nielsen, *J. Spectrosc.*, 2003, **17**, 787940.
14 F. Zhu, N. W. Isaacs, L. Hecht and L. D. Barron, *Structure*, 2005, **13**, 1409–1419.
15 F. Zhu, N. W. Isaacs, L. Hecht, G. E. Tranter and L. D. Barron, *Chirality*, 2006, **18**, 103–115.
16 C. Merten, H. Li, X. Lu, A. Hartwig and L. A. Nafie, *J. Raman Spectrosc.*, 2010, **41**, 1563–1565.
17 C. Merten, H. Li and L. A. Nafie, *J. Phys. Chem. A*, 2012, **116**, 7329–7336.
18 A. Kolodziejczyk, L. A. Nafie, A. Wajda and A. Kaczor, *Chem. Commun.*, 2023, **59**, 10793–10796.
19 L. A. Nafie, *Chem. Phys.*, 1996, **205**, 309–322.
20 M. Vargek, T. B. Freedman, E. Lee and L. A. Nafie, *Chem. Phys. Lett.*, 1998, **287**, 359–364.
21 M. Magg, Y. Kadria-Vili, P. Oulevey, R. B. Weisman and T. Bürgi, *J. Phys. Chem. Lett.*, 2016, **7**, 221–225.
22 T. Fujisawa, R. L. Leverenz, M. Nagamine, C. A. Kerfeld and M. Unno, *J. Am. Chem. Soc.*, 2017, **139**, 10456–10460.
23 T. Fujisawa, K. Nishikawa, J. Tamogami and M. Unno, *J. Phys. Chem. Lett.*, 2021, **12**, 9564–9568.
24 T. Fujisawa and M. Unno, *J. Phys. Chem. B*, 2024, **128**, 2228–2235.
25 S. Haraguchi, M. Hara, T. Shingae, M. Kumauchi, W. D. Hoff and M. Unno, *Angew. Chem., Int. Ed.*, 2015, **54**, 11555–11558.
26 S. Haraguchi, T. Shingae, T. Fujisawa, N. Kasai, M. Kumauchi, T. Hanamoto, W. D. Hoff and M. Unno, *Proc. Natl. Acad. Sci. U. S. A.*, 2018, **115**, 8671–8675.
27 J. Matsuo, T. Kikukawa, T. Fujisawa, W. D. Hoff and M. Unno, *J. Phys. Chem. Lett.*, 2020, **11**, 8579–8584.
28 K. Nishikawa, R. Kuroiwa, J. Tamogami, M. Unno and T. Fujisawa, *J. Phys. Chem. B*, 2023, **127**, 7244–7250.
29 M. Ohya, T. Kikukawa, J. Matsuo, T. Tsukamoto, R. Nagaura, T. Fujisawa and M. Unno, *J. Phys. Chem. B*, 2023, **127**, 4775–4782.
30 T. Shingae, K. Kubota, M. Kumauchi, F. Tokunaga and M. Unno, *J. Phys. Chem. Lett.*, 2013, **4**, 1322–1327.
31 M. Dudek, E. Machalska, T. Oleszkiewicz, E. Grzebelus, R. Baranski, P. Szcześniak, J. Mlynarski, G. Zajac, A. Kaczor and M. Baranska, *Angew. Chem., Int. Ed.*, 2019, **58**, 8383–8388.
32 M. Dudek, G. Zajac, A. Kaczor and M. Baranska, *J. Raman Spectrosc.*, 2017, **48**, 673–679.
33 N. Hachlica, M. Stefańska, M. Mach, M. Kowalska, P. Wydro, A. Domagała, J. Kessler, G. Zając and A. Kaczor, *Small*, 2024, **20**, e2306707.
34 J. Mazurkiewicz, E. Stanek, A. Kolodziejczyk, M. Karpiel, K. Czamara, T. H. Ferreira, P. Maximiano, P. N. Simões, I. Reva, J. Kalinowska-Tłuścik and A. Kaczor, *Phys. Chem. Chem. Phys.*, 2024, **26**, 7865–7876.
35 J. Mazurkiewicz, E. Stanek, P. Maximiano, T. H. Ferreira, M. Karpiel, S. Buda, J. Kalinowska-Tłuścik, P. N. N. L. Simões, I. Reva and A. Kaczor, *Phys. Chem. Chem. Phys.*, 2025, **27**, 4905–4914.
36 A. Orlef, E. Stanek, K. Czamara, A. Wajda and A. Kaczor, *Chem. Commun.*, 2022, **58**, 9022–9025.
37 G. Zajac, A. Kaczor, S. Buda, J. Młynarski, J. Frelek, J. C. Dobrowolski and M. Baranska, *J. Phys. Chem. B*, 2015, **119**, 12193–12201.
38 G. Zajac, A. Kaczor, A. Pallares Zazo, J. Mlynarski, M. Dudek and M. Baranska, *J. Phys. Chem. B*, 2016, **120**, 4028–4033.
39 J. Bogaerts and C. Johannessen, *J. Raman Spectrosc.*, 2019, **50**, 641–646.
40 E. Machalska, G. Zajac, A. Gruca, F. Zobi, M. Baranska and A. Kaczor, *J. Phys. Chem. Lett.*, 2020, **11**, 5037–5043.
41 R. Sgammato, W. Herrebout and C. Johannessen, *J. Raman Spectrosc.*, 2019, **50**, 1905–1913.
42 T. Wu, G. Li, J. Kapitán, J. Kessler, Y. Xu and P. Bouř, *Angew. Chem., Int. Ed.*, 2020, **59**, 21895–21898.
43 G. Li, M. Alshalalfeh, J. Kapitán, P. Bouř and Y. Xu, *Chem. – Eur. J.*, 2022, **28**(20), e202104302.
44 G. Li, M. Alshalalfeh, Y. Yang, J. R. Cheeseman, P. Bouř and Y. Xu, *Angew. Chem., Int. Ed.*, 2021, **60**, 22004–22009.
45 E. Machalska, G. Zajac, A. J. Wierzba, J. Kapitán, T. Andruniów, M. Spiegel, D. Gryko, P. Bouř and M. Baranska, *Angew. Chem., Int. Ed.*, 2021, **60**, 21205–21210.
46 E. Machalska, N. Hachlica, G. Zajac, D. Carraro, M. Baranska, G. Licini, P. Bouř, C. Zonta and A. Kaczor, *Phys. Chem. Chem. Phys.*, 2021, **23**, 23336–23340.
47 T. Wu, J. Kapitán and P. Bouř, *J. Phys. Chem. Lett.*, 2022, **13**, 3873–3877.
48 J. Mazurkiewicz, A. Orlef, T. Misiaszek, T. K. Olszewski and A. Kaczor, *Chem. Commun.*, 2025, **61**, 5954–5957.
49 M. Dudek, G. Zajac, A. Kaczor and M. Baranska, *J. Phys. Chem. B*, 2016, **120**, 7807–7814.
50 G. Zajac, J. Lasota, M. Dudek, A. Kaczor and M. Baranska, *Spectrochim. Acta, Part A*, 2017, **173**, 356–360.
51 M. Halat, G. Zając, V. Andrushchenko, P. Bouř, R. Baranski, K. Pajor and M. Baranska, *Angew. Chem., Int. Ed.*, 2024, **63**, e202402449.
52 J. Langer, D. J. de Aberasturi, J. Aizpurua, R. A. Alvarez-Puebla, B. Auguié, J. J. Baumberg, G. C. Bazan, S. E. J. Bell, A. Boisen, A. G. Brolo, J. Choo, D. Cialla-May, V. Deckert, L. Fabris, K. Faulds, F. Javier García de Abajo, R. Goodacre, D. Graham, A. J. Haes, C. L. Haynes, C. Huck, T. Itoh, M. Käll, J. Kneipp, N. A. Kotov, H. Kuang, E. C. Le Ru, H. K. Lee, J. F. Li, X. Y. Ling, S. A. Maier, T. Mayerhöfer, M. Moskovits, K. Murakoshi, J. M. Nam, S. Nie, Y. Ozaki, I. Pastoriza-Santos, J. Perez-Juste, J. Popp, A. Pucci, S. Reich, B. Ren, G. C. Schatz, T. Shegai, S. Schlücker, L. L. Tay, K. George Thomas, Z. Q. Tian, R. P. van Duyne, T. Vo-Dinh, Y. Wang, K. A. Willets, C. Xu, H. Xu, Y. Xu, Y. S. Yamamoto, B. Zhao and L. M. Liz-Marzán, *ACS Nano*, 2020, **14**, 28–117.
53 S. Abdali and E. W. Blanch, *Chem. Soc. Rev.*, 2008, **37**, 980–992.
54 S. Ostovar Pour, L. D. Barron, S. T. Mutter and E. W. Blanch, *Chiral Analysis*, ed. P. L. Polavarapu, Elsevier, 2nd edn, 2018, pp. 249–291, DOI: **10.1016/B978-0-444-64027-7.00006-9**.
55 S. Abdali, C. Johannessen, J. Nygaard and T. Nørbygaard, *J. Phys.: Condens. Matter*, 2007, **19**, 285205.
56 C. Johannessen, P. C. White and S. Abdali, *J. Phys. Chem. A*, 2007, **111**, 7771–7776.
57 S. Abdali, *J. Raman Spectrosc.*, 2006, **37**, 1341–1345.
58 H. Kneipp, J. Kneipp and K. Kneipp, *Anal. Chem.*, 2006, **78**, 1363–1366.
59 S. O. Pour, S. E. J. Bell and E. W. Blanch, *Chem. Commun.*, 2011, **47**, 4754–4756.
60 M. Das, D. Gangopadhyay, J. Šebestík, L. Habartová, P. Michal, J. Kapitán and P. Bouř, *Chem. Commun.*, 2021, **57**, 6388–6391.
61 M. Das, D. Gangopadhyay, V. Andrushchenko, J. Kapitán and P. Bouř, *ACS Nano*, 2025, **19**, 10412–10420.

Open Access Article. Published on 02 2025. Downloaded on 06.02.2026 19:38:33.
This article is licensed under a Creative Commons Attribution 3.0 Unported Licence.

62 S. Ostovar Pour, L. Rocks, K. Faulds, D. Graham, V. Parchaňský, P. Bouř and E. W. Blanch, *Nat. Chem.*, 2015, **7**, 591–596.
63 K. Hiramatsu, H. Kano and T. Nagata, *Opt. Express*, 2013, **21**, 13515–13521.
64 L. A. Nafie, in *Frontiers and Advances in Molecular Spectroscopy*, ed. J. Laane, Elsevier, 2018, pp. 421–469, DOI: 10.1016/B978-0-12-811220-5.00014-9.
65 K. Hiramatsu, M. Okuno, H. Kano, P. Leproux, V. Couderc and H.-O. Hamaguchi, *Phys. Rev. Lett.*, 2012, **109**, 083901.
66 K. Hiramatsu, P. Leproux, V. Couderc, T. Nagata and H. Kano, *Opt. Lett.*, 2015, **40**, 4170–4173.
67 V. Kumar, T. Reichenauer, L. Supovec, D. Jansen, N. Brodt, G. Zając, A. Domagała, M. Barańska, J. Niemeyer and S. Schlücker, *J. Raman Spectrosc.*, 2023, **54**, 1011–1020.
68 D. Kurouski, X. Lu, L. Popova, W. Wan, M. Shanmugasundaram, G. Stubbs, R. K. Dukor, I. K. Lednev and L. A. Nafie, *J. Am. Chem. Soc.*, 2014, **136**, 2302–2312.
69 P. C. Ke, R. Zhou, L. C. Serpell, R. Riek, T. P. J. Knowles, H. A. Lashuel, E. Gazit, I. W. Hamley, T. P. Davis, M. Fändrich, D. E. Otzen, M. R. Chapman, C. M. Dobson, D. S. Eisenberg and R. Mezzenga, *Chem. Soc. Rev.*, 2020, **49**, 5473–5509.
70 S. Mankar, A. A. S. Shamik and S. K. Maji, *Nano Rev.*, 2011, **2**, 6032.
71 E. W. Blanch, L. A. Morozova-Roche, D. A. Cochran, A. J. Doig, L. Hecht and L. D. Barron, *J. Mol. Biol.*, 2000, **301**, 553–563.
72 E. Tayeb-Fligelman, O. Tabachnikov, A. Moshe, O. Goldshmidt-Tran, M. R. Sawaya, N. Coquelle, J.-P. Colletier and M. Landau, *Science*, 2017, **355**, 831–833.
73 J. Adamcik and R. Mezzenga, *Angew. Chem., Int. Ed.*, 2018, **57**, 8370–8382.
74 N. Rubin, E. Perugia, M. Goldschmidt, M. Fridkin and L. Addadi, *J. Am. Chem. Soc.*, 2008, **130**, 4602–4603.
75 N. Hachlica, M. Rawski, M. Górecki, A. Wajda and A. Kaczor, *Chem – Eur. J.*, 2023, **29**(30), e202203827.
76 D. Kurouski, R. K. Dukor, X. F. Lu, L. A. Nafie and I. K. Lednev, *Biophys. J.*, 2012, **103**, 522–531.
77 D. Kurouski, R. A. Lombardi, R. K. Dukor, I. K. Lednev and L. A. Nafie, *Chem. Commun.*, 2010, **46**, 7154–7156.
78 Y. Cao, J. Adamcik, M. Diener, J. R. Kumita and R. Mezzenga, *J. Am. Chem. Soc.*, 2021, **143**, 11473–11481.
79 A. Saiani, A. Mohammed, H. Frielinghaus, R. Collins, N. Hodson, C. M. Kielty, M. J. Sherratt and A. F. Miller, *Soft Matter*, 2009, **5**, 193–202.
80 L. D. Barron, L. Hecht, E. W. Blanch and A. F. Bell, *Prog. Biophys. Mol. Biol.*, 2000, **73**, 1–49.
81 T. A. Keiderling, *Curr. Opin. Chem. Biol.*, 2002, **6**, 682–688.
82 T. A. Keiderling, *Chem. Rev.*, 2020, **120**, 3381–3419.
83 V. P. Nicu, *Phys. Chem. Chem. Phys.*, 2016, **18**, 21202–21212.
84 V. P. Nicu, *Phys. Chem. Chem. Phys.*, 2016, **18**, 21213–21225.
85 T. J. Measey and R. Schweitzer-Stenner, *J. Am. Chem. Soc.*, 2011, **133**, 1066–1076.
86 W. R. W. Welch, J. Kubelka and T. A. Keiderling, *J. Phys. Chem. B*, 2013, **117**, 10343–10358.
87 N. O'Neill, T. A. Lima, F. F. Ferreira, L. Thursch, N. Alvarez and R. Schweitzer-Stenner, *J. Phys. Chem. B*, 2022, **126**, 8080–8093.
88 N. O'Neill, T. A. Lima, F. Furlan Ferreira, N. J. Alvarez and R. Schweitzer-Stenner, *Spectrochim. Acta, Part A*, 2024, **306**, 123584.
89 A. Kaczor, *Phys. Chem. Chem. Phys.*, 2023, **25**, 19371–19379.
90 Z. Majka, K. Kwiecień and A. Kaczor, *ChemPlusChem*, 2024, **89**, e202400091.
91 S. L. Ma, X. L. Cao, M. Mak, A. Sadik, C. Walkner, T. B. Freedman, I. K. Lednev, R. K. Dukor and L. A. Nafie, *J. Am. Chem. Soc.*, 2007, **129**, 12364–12365.
92 C. D. Syme, E. W. Blanch, C. Holt, R. Jakes, M. Goedert, L. Hecht and L. D. Barron, *Eur. J. Biochem.*, 2002, **269**, 148–156.
93 S. Yamamoto and H. Watarai, *Chirality*, 2012, **24**, 97–103.
94 J. Kessler, S. Yamamoto and P. Bouř, *Phys. Chem. Chem. Phys.*, 2017, **19**, 13614–13621.
95 X. Lu, H. Li, J. W. Nafie, T. Pazderka, M. Pazderková, R. K. Dukor and L. A. Nafie, *Appl. Spectrosc.*, 2017, **71**, 1117–1126.
96 A. Micsonai, F. Wien, L. Kernya, Y.-H. Lee, Y. Goto, M. Réfrégiers and J. Kardos, *Proc. Natl. Acad. Sci. U. S. A.*, 2015, **112**, E3095–E3103.
97 C. R. Lightner, A. Kaczor and C. Johannessen, *Vib. Spectrosc.*, 2024, **132**, 103683.
98 N. Hachlica, A. Kolodziejczyk, M. Rawski, M. Górecki, A. Wajda and A. Kaczor, *Spectrochim. Acta, Part A*, 2024, **304**, 123293.
99 M. G. Iadanza, M. P. Jackson, E. W. Hewitt, N. A. Ranson and S. E. Radford, *Nat. Rev. Mol. Cell Biol.*, 2018, **19**, 755–773.
100 N. Louros, J. Schymkowitz and F. Rousseau, *Nat. Rev. Mol. Cell Biol.*, 2023, **24**, 912–933.
101 A. T. Petkova, R. D. Leapman, Z. H. Guo, W. M. Yau, M. P. Mattson and R. Tycko, *Science*, 2005, **307**, 262–265.
102 A. Bansal, M. Schmidt, M. Rennegarbe, C. Haupt, F. Liberta, S. Stecher, I. Puscalau-Girtu, A. Biedermann and M. Fändrich, *Nat. Commun.*, 2021, **12**, 1013.
103 S. Lövestam, M. Schweighauser, T. Matsubara, S. Murayama, T. Tomita, T. Ando, K. Hasegawa, M. Yoshida, A. Tarutani, M. Hasegawa, M. Goedert and S. H. W. Scheres, *FEBS open bio*, 2021, **11**, 999–1013.
104 M. Zielinski, C. Röder and G. F. Schröder, *J. Biol. Chem.*, 2021, **297**, 100938.
105 C. Soto and S. Pritzkow, *Nat. Neurosci.*, 2018, **21**, 1332–1340.

 This journal is © The Royal Society of Chemistry 2025